Plasmonic enhancement of electroluminescence

D. V. Guzatov, S. V. Gaponenko, and H. V. Demir

Citation: AIP Advances **8**, 015324 (2018);
View online: https://doi.org/10.1063/1.5019778
View Table of Contents: http://aip.scitation.org/toc/adv/8/1
Published by the American Institute of Physics

Plasmonic enhancement of electroluminescence

D. V. Guzatov,[1] S. V. Gaponenko,[2,a] and H. V. Demir[3,4]
[1]*Yanka Kupala Grodno State University, Grodno 230023, Belarus*
[2]*B. I. Stepanov Institute of Physics, National Academy of Sciences, Minsk 220072, Belarus*
[3]*Department of Electrical and Electronics Engineering, Department of Physics, and UNAM–Institute of Materials Science and Nanotechnology, Bilkent University, Ankara 06800, Turkey*
[4]*LUMINOUS! Center of Excellence for Semiconductor Lighitng and Displays, School of Electrical and Electronic Engineering, School of Physical and Mathematical Sciences, Nanyang Technological University, 50 Nanyang Ave 639798, Singapore*

(Received 16 December 2017; accepted 15 January 2018; published online 24 January 2018)

Here plasmonic effect specifically on electroluminescence (EL) is studied in terms of radiative and nonradiative decay rates for a dipole near a metal spherical nanoparticle (NP). Contribution from scattering is taken into account and is shown to play a decisive role in EL enhancement owing to pronounced size-dependent radiative decay enhancement and weak size effect on non-radiative counterpart. Unlike photoluminescence where local incident field factor mainly determines the enhancement possibility and level, EL enhancement is only possible by means of quantum yield rise, EL enhancement being feasible only for an intrinsic quantum yield $Q_0 < 1$. The resulting plasmonic effect is independent of intrinsic emitter lifetime but is exclusively defined by the value of Q_0, emission spectrum, NP diameter and emitter-metal spacing. For $0.1 < Q_0 < 0.25$, Ag nanoparticles are shown to enhance LED/OLED intensity by several times over the whole visible whereas Au particles feature lower effect within the red-orange range only. Independently of positive effect on quantum yield, metal nanoparticles embedded in an electroluminescent device will improve its efficiency at high currents owing to enhanced overall recombination rate which will diminish manifestation of Auger processes. The latter are believed to be responsible for the known undesirable efficiency droop in semiconductor commercial quantum well based LEDs at higher current. For the same reason plasmonics can diminish quantum dot photodegradation from Auger process induced non-radiative recombination and photoionization thus opening a way to avoid negative Auger effects in emerging colloidal semiconductor LEDs. https://doi.org/10.1063/1.5019778

I. INTRODUCTION

Plasmonic luminescence enhancement has become an active field of research because of potential applications in lighting, display and analytical devices.[1–5] Till recently only *photo*luminescence enhancement by metal nanoparticles (NP) has been examined and many groups have experimentally demonstrated photoluminescence intensity enhancement for molecular and semiconductor emitters (Refs. 6–12 and Refs. therein) using Ag and Au nanostructures. In simple cases of an emitter with high intrinsic quantum yield $Q_0 \approx 1$ and spherical metal particles, typical enhancement factors of the order of 10 are reported whereas specially designed nanostructures (arrays, nanoshells and nanoantennas) make higher enhancement factors feasible.[8–10] For photoluminescence modified by plasmonic effects, intensity is defined by excitation rate of an emitter and its quantum yield Q affected by a metal NP, a nanoantenna, or an array of nanobodies. For emitters with high intrinsic quantum yield in typical experiments $Q < Q_0$ holds since enhancement of nonradiative decay component dominates over the

[a]To whom correspondence should be addressed, e-mail s.gaponenko@ifanbel.bas-net.by

radiative one.[11] Therefore, local incident field enhancement which in certain structures may locally experience 10^2-10^3 enhancement (i. e. 10^4-10^6 intensity enhancement, see Ref. 13 and Refs. therein) becomes the major factor enabling *photo*luminescence intensity increase. For emitters with intrinsically low Q_0 the relative growth of nonradiative transitions rate near a metal NP is not pronounced and much higher enhancement factors (to 10^3) become affordable for photoluminescence.[10] In the context of extensive progress in semiconductor light-emitting diodes (LEDs) and organic ones (OLEDs), positive effect from metal NPs embedded therein is challenging. Unlike photoluminescence, for *electro*luminescence, plasmonic effect reduces to a modified quantum yield, i. e., to a modified ratio of radiative versus nonradiative decay components. The desirable electroluminescence enhancement then becomes possible only for emitters with a lower intrinsic quantum yield $Q_0 < 1$. This circumstance has been highlighted in the early theoretical simulations[14] but a systematic theoretical analysis of plasmonic effect on quantum yield has not been reported to date. At the same time, a number of recent experiments[15–21] point out that plasmonics can enhance OLED[15,16] and LED performance including both quantum well based ones[17,21,22] and colloidal quantum dot based LEDs,[18–20] the latter being of special interest in the context of the colloidal nanophotonics platform[23,24] since metal NPs can be readily integrated therein.

In this paper, modeling of plasmonic effects in EL structures is reported based on the model of light emission by a dipole near a metal spherical NP. The model accounts for the scattering contribution that has been shown[11] to become crucial for NPs bigger than 20 nm, i.e. for the most of typical experimental situations. We show that it is scattering size-dependent extinction band that enables the desirable electroluminescence intensity enhancement through quantum yield increase. The multi-parametric problem is examined including the material type (Au and Ag), NP size, metal-emitter spacing, emission wavelength, and intrinsic quantum yield. The results obtained are in the reasonable agreement with the experiments and indicate possible intensity enhancement of LEDs and OLEDs by the factor of 1.5. . .5, being more pronounced for intrinsic quantum yield $Q_0 < 0.5$ and existing within the visible for Ag and only within orange-red spectrum for Au.

II. RESULTS AND DISCUSSION

A. The model

We use the approach[25] based on a modified radiative decay rate of a dipole emitter near a metal nanobody by means of computing its modified dipole transitions probability. The calculation scheme has been described elsewhere.[11] The most favorable case is considered of a dipole moment oriented along the line connecting an emitter with a NP center. The electroluminescence intensity enhancement factor F, i. e., change in the emission intensity I near metal versus intensity I_0 without metal equals the quantum yield change, reads,

$$F = \frac{I}{I_0} = \frac{Q}{Q_0} = \frac{\gamma_r}{\gamma_r + \gamma_{nr} + \gamma_{int}} \cdot \frac{\gamma_0 + \gamma_{int}}{\gamma_0} = \frac{\gamma_r}{\gamma_0} / \left[1 + Q_0 \left(\frac{\gamma_r + \gamma_{nr}}{\gamma_0} - 1\right)\right], \quad (1)$$

where

$$Q = \frac{\gamma_r}{\gamma_r + \gamma_{nr} + \gamma_{int}}, \quad Q_0 = \frac{\gamma_0}{\gamma_0 + \gamma_{int}}, \quad (2)$$

are the emitter quantum yield in the presence of a metal nanoparticle and in free space, respectively, γ_0 is the intrinsic radiative spontaneous decay rate, γ_{int} is the intrinsic nonradiative decay rate describing internal losses of an emitter, γ_r and γ_{nr} are the radiative and nonradiative decay rates of an emitter in the presence of a metal nanobody, respectively. The notion of quantum yield used here is the same as in photoluminescence. It is defined by the ratio of the radiative decay rate to the full decay rate of an emitter and in the case of a quantum well and a quantum dot equals the average number of emitted photons per single injected electron-hole pair. Since we do not consider injection process here, the quantum yield is the intrinsic property of an emitter without current flow arrangement and therefore, it is higher than the internal quantum efficiency (IQE) used in LED and laser diodes theory.

Since we consider that Q_0 is known, it is convenient to write nonradiative decay rate as $\gamma_{int} = \gamma_0(1/Q_0 - 1)$. Then calculations reduce to computation of the two values, γ_r/γ_0 and $(\gamma_r + \gamma_{nr})/\gamma_0$.

For the dipole orientation chosen the required values read[2,11,26]

$$\frac{\gamma_r}{\gamma_0} = \frac{3}{2}\sum_{n=1}^{\infty} n\,(n+1)\,(2n+1)\left|\frac{\psi_n\,(k_0 r_0)}{(k_0 r_0)^2} + A_n\frac{\zeta_n\,(k_0 r_0)}{(k_0 r_0)^2}\right|^2, \tag{3}$$

$$\frac{\gamma_r + \gamma_{nr}}{\gamma_0} = 1 + \frac{3}{2}\sum_{n=1}^{\infty} n\,(n+1)\,(2n+1)\,\mathrm{Re}\left\{A_n\left(\frac{\zeta_n\,(k_0 r_0)}{(k_0 r_0)^2}\right)^2\right\}, \tag{4}$$

where $\psi_n(x) = xj_n(x)$ and $\zeta_n\,(x) = xh_n^{(1)}\,(x)$ are Ricatti–Bessel functions, $j_n(x)$ and $h_n^{(1)}\,(x)$ are the spherical Bessel functions, k_0 is wave number in vacuum, $r_0 = a + \Delta r$ is distance for an NP center to an emitter, and

$$A_n = -\left(\frac{\sqrt{\varepsilon}\psi_n\left(k_0 a\sqrt{\varepsilon}\right)\psi_n'\,(k_0 a) - \psi_n'\left(k_0 a\sqrt{\varepsilon}\right)\psi_n\,(k_0 a)}{\sqrt{\varepsilon}\psi_n\left(k_0 a\sqrt{\varepsilon}\right)\zeta_n'\,(k_0 a) - \psi_n'\left(k_0 a\sqrt{\varepsilon}\right)\zeta_n\,(k_0 a)}\right) \tag{5}$$

is one of the Mie coefficients for the field reflected from a NP surface, primes denote derivatives, a is NP radius, and ε is the metal complex dielectric permittivity. When an emitter is moved far from the metal NP, i.e. when $k_0 r_0 \to \infty$ holds, one has $\gamma_r/\gamma_0 \to 1$ and $(\gamma_r + \gamma_{nr})/\gamma_0 \to 1$, and then $Q \to Q_0$ is the case. Eqs. (3), (4) allow to calculate the electroluminescence intensity enhancement factor (1). Notably, Eqs. (1)–(5) show that plasmonic effect on electroluminescence intensity does not depend on the absolute values of intrinsic radiative γ_0 and nonradiative γ_{int} decay rates, i. e., it is independent of intrinsic emitter lifetime $\tau = (\gamma_0 + \gamma_{int})^{-1}$. Enhancement/quenching is entirely defined by Q_0, emission spectrum, metal dielectric permittivity, nanoparticle size, and emitter—metal spacing. Calculations were made for 20. . .80 nm Ag and Au NPs with $\varepsilon(\lambda)$ function according to Ref. 27. The range $Q_0 = 0.1...0.5$ was chosen since lower values make emitters inefficient for commercial lighting and higher values do not allow for plasmonic enhancement in most of the practical cases.

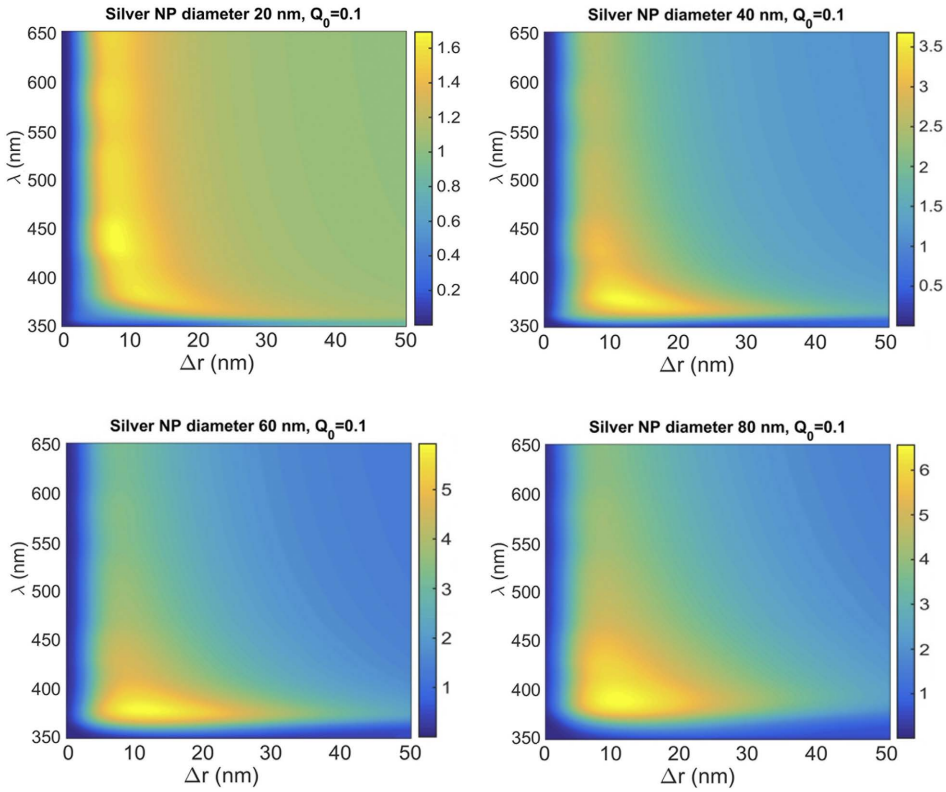

FIG. 1. Calculated enhancement of electroluminescence intensity for an emitter with intrinsic quantum yield 0.1 near an Ag nanoparticle with diameter 20, 40, 60, and 80 nm. Ambient medium refraction index is equal to 1.

B. Enhancement factors for Ag nanoparticles

Figs. 1–3 show modification of EL intensity for Ag nanoparticles as a function of the emission wavelength and spacing $\Delta r = r_0 - a$. One can see that calculations predict higher enhancement for lower Q_0 and bigger nanoparticles. It is noteworthy that the enhancement is feasible within a wide spectral range λ = 400-650 nm covering the blue, green and red and therefore can be used in lighting and display devices. The maximal calculated enhancement reaches 5-6 times, for the optimal emitter—metal spacing being 8-15 nm.

Calculations show that enhancement factor is higher for lower intrinsic quantum yield Q_0, the maximal Q obtained in calculation is about 0.6-0.8 and does not reach 1. There is pronounced tendency to higher enhancement for bigger nanoparticle size. This correlation has the reasonable physical background.

C. Correlation of the enhancement factor with extinction spectrum

The apparent size dependence of the enhancement factor results from the two regularities. First, for the electroluminescence intensity enhancement to become possible, radiative decay enhancement should dominate over nonradiative counterpart (luminescence quenching by a metal proximity). This is typically performed by choosing the proper distance since quenching rapidly vanishes with distance and is negligible at metal-emitter spacing more than 20 nm. Second, and even more important, is the fact that radiative decay enhancement spectrum directly correlates with the extinction spectrum whereas quenching does not. The latter is mainly defined by the dielectric function spectrum, i. e., it is defined chiefly by the metal type rather than metal nanobody size (and shape). Radiative decay enhancement is defined by the local photon density of states (DOS) which correlates with the incident field enhancement, the latter in its turn being directly related with metal nanoparticles extinction spectrum. When nanoparticles size cannot be neglected as compared to radiation wavelength, the

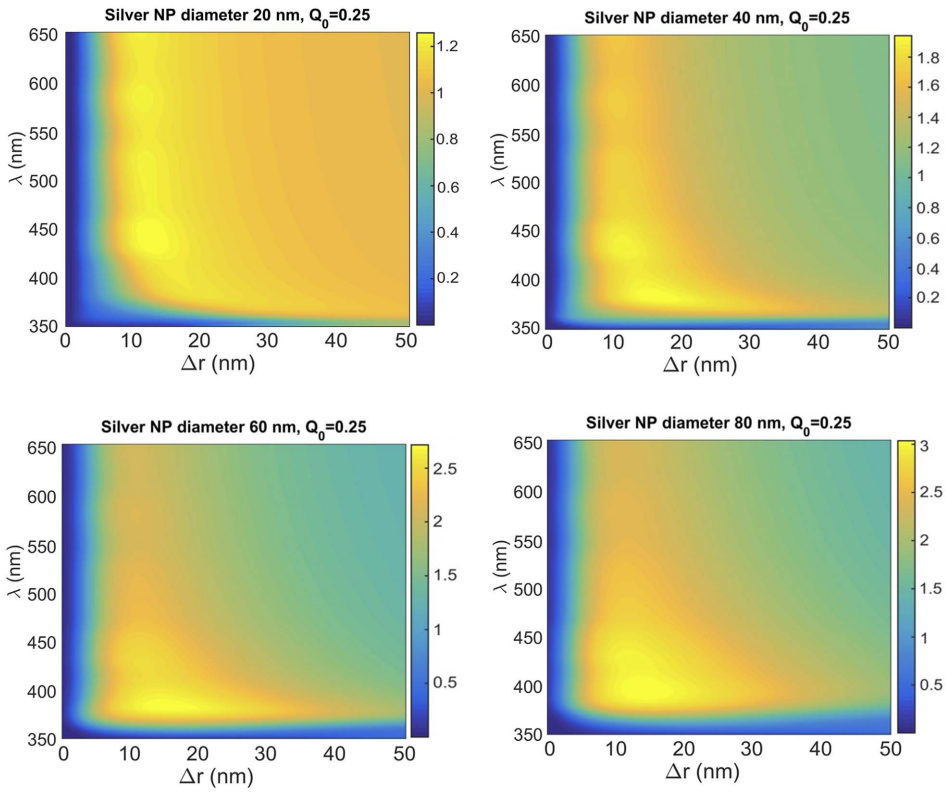

FIG. 2. Calculated enhancement of electroluminescence intensity for an emitter with intrinsic quantum yield 0.25 near an Ag nanoparticle with diameter 20, 40, 60, and 80 nm.

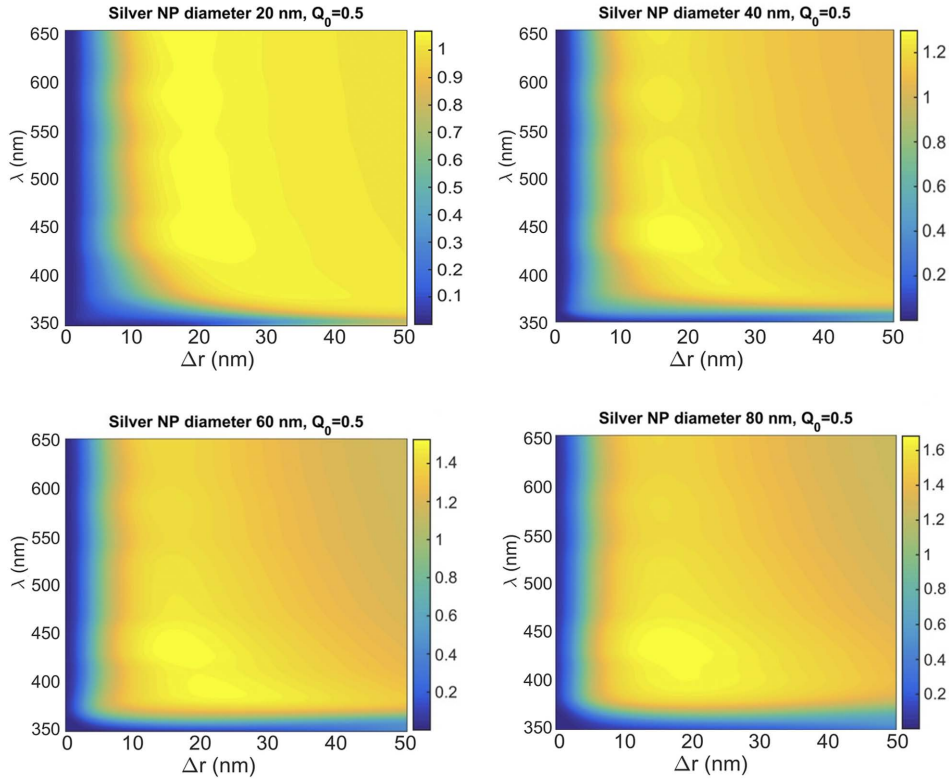

FIG. 3. Calculated enhancement of electroluminescence intensity for an emitter with intrinsic quantum yield 0.5 near an Ag nanoparticle with diameter 20, 40, 60, and 80 nm.

size-dependent extinction band develops moving to longer wavelengths and getting wider with increasing size as shown in Fig. 4.

One can see that enhancements plotted in Figs. 1–3 result from radiative decay enhancement tailored by the size-dependent extinction spectrum. For example, for emission wavelengths 450-460 nm (the principal emission wavelength of blue LEDS used in lighting) radiative decay enhancement factor grows monotonically by a factor of 6-8 whereas the same value for nonradiative rate changes by the factor less than 2. This property allows for spectral separation of competitive radiative and nonradiative factors and becomes the decisive factor in obtaining electroluminescence enhancement by means of plasmonics. Taking into account that extinction spectrum can be shifted away from the dielectric permittivity one not only by size increase we expect that similar behavior will occur for

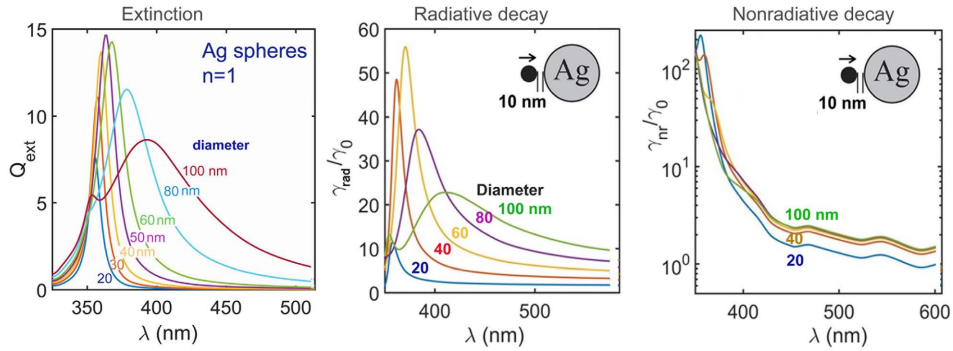

FIG. 4. Extinction spectrum, radiative decay rate enhancement, and nonradiative decay rate enhancement spectra for Ag nanoparticles with diameter ranging from 20 to 100 nm and metal emitter spacing 10 nm. Ambient medium refractive index equals 1.

elongated particles (as has been shown in Refs. 28,29) and also for metal nanoparticles embedded in an ambient material with refractive index $n_m > 1$. The latter corresponds to decrease of radiation wavelength in the ambient medium as compared to nanobody size thus resulting in enhanced scattering which in turn leads to higher extinction.

D. Ambient medium refractive index effect

Calculations for ambient medium refractive index $n_m > 1$ reduce to substitution of $k_0 n_m$ instead of k_0 and ε/n_m^2 instead of ε in Eqs. (3)–(5). In Fig. 5 selected results for electroluminescence intensity enhancement by silver nanoparticles of different sizes in the medium with refractive index 1.5 which is typical for polymers. Comparing Fig. 5 with Figs. 1, 2, one can see that the long-wave spectral shift of enhancement range exists for higher refractive index which correlates with the shift of extinction spectrum (not shown). Note that higher refractive index results in higher enhancement factors, especially in the long-wave range. These features result from interplay of refractive index effects on light scattering, extinction spectrum, decay rates. At the same time, enhancement occurs for shorter metal-emitter spacing ($\Delta r < 5$ nm) which can be interpreted as a result of the n factor for $r_0 = a + \Delta r$ in Eqs. (3), (4).

When considering impact of ambient medium refractive index one should bear in mind that Q_0 now is to be treated not as emitter quantum yield in vacuum but as quantum yield modified owing to ambient medium effect. Radiative decay rate typically rise up for $n_m > 1$ (see, e. g., Ref. 3, Chapter 14), though different emitter type (an atom, a molecule, a quantum dot, a quantum well) may exhibit different radiative decay rate dependence on n_m because of specific local field corrections involved. Thus, when considering the plasmonic effect on quantum yield in a refractive medium with respect to vacuum it will be even higher than that shown in Fig. 5.

E. Averaging over emitter orientations

The above results correspond to an idealized case of the optimal emitter dipole moment orientation with respect to a metal nanoparticle (inserts in Fig. 4). In real situations random orientation

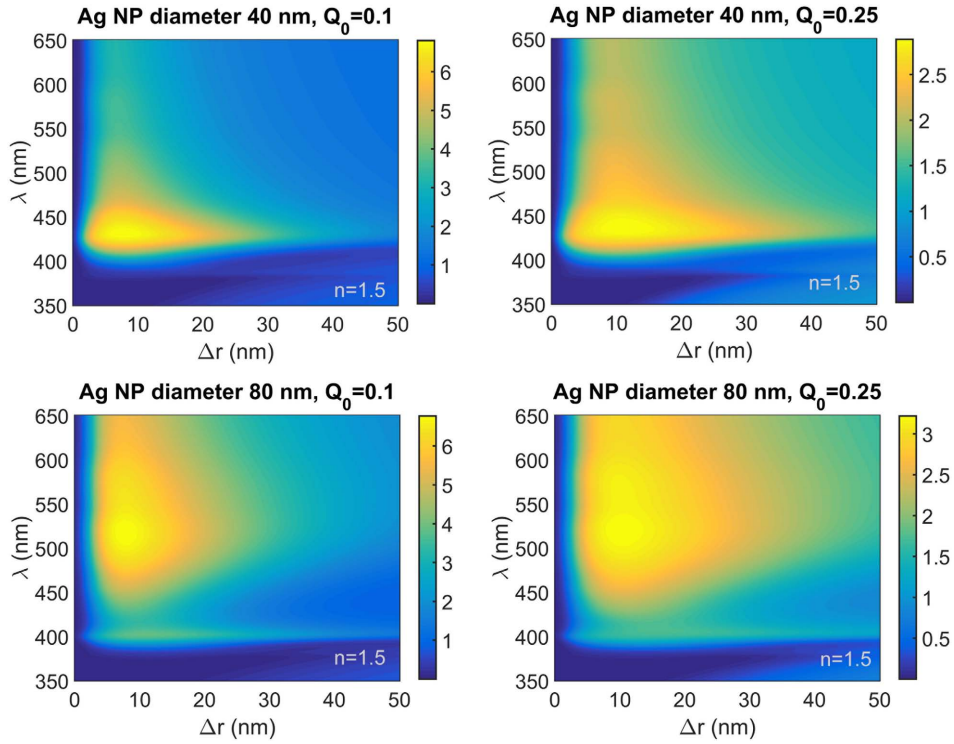

FIG. 5. Calculated enhancement of electroluminescence intensity for ambient medium refraction index 1.5 for Ag nanoparticle diameter (top panels) 40 and (bottom panels) 80 nm, and intrinsic quantum yield $Q_0 = 0.1$ (left) and 0.25 (right).

of dipoles is very probable and then the actual enhancement will be lower. To account for random orientation impact on enhancement of electroluminescence intensity, the following relation was used,

$$\langle F\rangle = \langle Q\rangle / Q_0, \quad \langle Q\rangle = \frac{1}{3}\left(Q_{norm} + 2Q_{tang}\right), \tag{6}$$

where subscript "norm" and "tang" correspond to the normal and tangential dipole moment orientation, respectively. Q_{tang} has been calculated using the following relations (cf (2)–(5))[2,11,26]

$$Q_{tang} = \left.\frac{\gamma_r}{\gamma_r + \gamma_{nr} + \gamma_{int}}\right|_{tang}, \tag{7}$$

where (in vacuum)

$$\left.\frac{\gamma_r}{\gamma_0}\right|_{tang} = \frac{3}{4}\sum_{n=1}^{\infty}(2n+1)\left(\left|\frac{\psi_n(k_0r_0)}{k_0r_0} + B_n\frac{\zeta_n(k_0r_0)}{k_0r_0}\right|^2 + \left|\frac{\psi_n'(k_0r_0)}{k_0r_0} + A_n\frac{\zeta_n'(k_0r_0)}{k_0r_0}\right|^2\right), \tag{8}$$

$$\left.\frac{\gamma_r + \gamma_{nr}}{\gamma_0}\right|_{tang} = 1 + \frac{3}{4}\sum_{n=1}^{\infty}(2n+1)\,\mathrm{Re}\left\{B_n\left(\frac{\zeta_n(k_0r_0)}{k_0r_0}\right)^2 + A_n\left(\frac{\zeta_n'(k_0r_0)}{k_0r_0}\right)^2\right\}, \tag{9}$$

and

$$B_n = -\left(\frac{\psi_n\left(k_0a\sqrt{\varepsilon}\right)\psi_n'(k_0a) - \sqrt{\varepsilon}\psi_n'\left(k_0a\sqrt{\varepsilon}\right)\psi_n(k_0a)}{\psi_n\left(k_0a\sqrt{\varepsilon}\right)\zeta_n'(k_0a) - \sqrt{\varepsilon}\psi_n'\left(k_0a\sqrt{\varepsilon}\right)\zeta_n(k_0a)}\right). \tag{10}$$

Note that for ambient medium refractive index $n_{\text{m}} > 1$ substitutions of k_0n_m instead of k_0 and ε/n_m^2 instead of ε should be made. Calculation of Q_{norm} can be done according to (1)–(5) with the above substitutions.

The representative example of orientation effect is shown in Fig. 6 for refractive index 1.5 and nanoparticle diameter 60 nm. One can see that even the most unfavorable tangential orientation of the emitter dipole moment still promise enhancement factor about 2 for intrinsic quantum yield 0.25 and 60 nm Ag particle diameter in the most critical spectral range of commercial InGaN LEDs used in white LED for lighting. Random orientation offers more than 2-fold enhancement in the same spectral range.

F. Comparison of Au and Ag effects

Calculations for Au nanoparticles have shown that the enhancement is possible within the red-orange range and for $Q_0 > 0.2$ it tends to vanish. Therefore, in Fig. 7, data are presented for Au nanoparticles for $Q_0 = 0.1$ only. The optimal spacing is 10-35 nm. Different spectral features for Ag and Au come from spectral behavior of nonradiative decay rate γ_{nr} which dominates over radiative one for Au particles in wide spectral range. This is shown in Fig. 8 where relatively large metal-emitter spacing (25 nm) has been chosen to minimize non-desirable nonradiative enhancement factor. (Fig. 8).

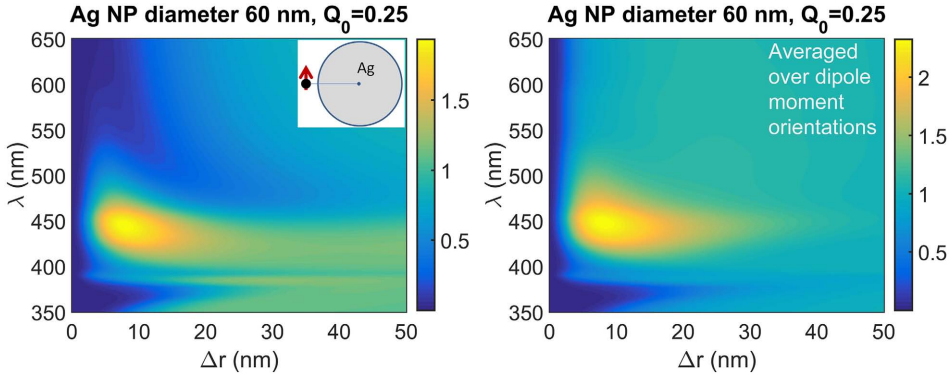

FIG. 6. Electroluminescence enhancement by 60 nm Ag particles for (left) tangential and (right) random averaged orientation of the emitter dipole moment.

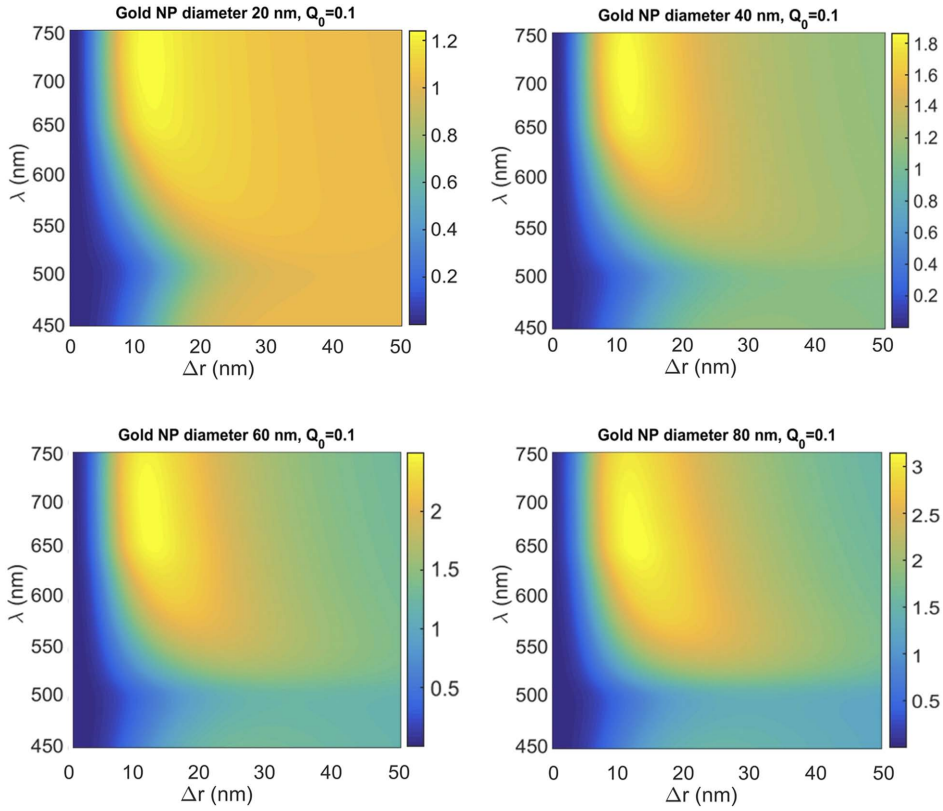

FIG. 7. Calculated enhancement of electroluminescence intensity for an emitter with intrinsic quantum yield 0.1 near an Au nanoparticle with diameter 20, 40, 60, and 80 nm. Ambient medium refractive index is 1.

For both metals the favorable radiative rate enhancement correlates with extinction spectrum which in turn correlates with $\varepsilon(\lambda)$ dependence, which features the narrow maximum in the near UV-range for Ag and smooth behavior for Au in the wide range. For this reason Au NPs are efficient only for wavelengths longer than 550 nm and cannot be used for commercial blue LEDs. However Au nanoparticles can be useful to enhance color converting phosphor performance in white LED but this issue is beyond the scope of the paper.

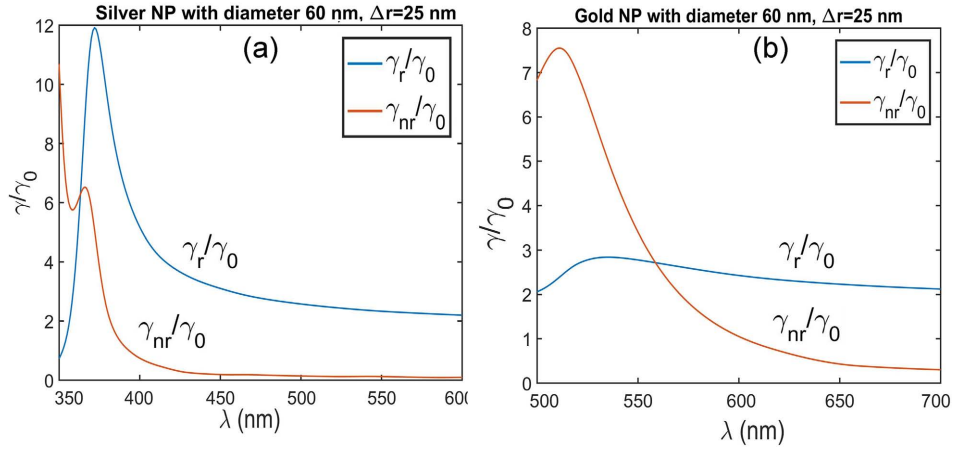

FIG. 8. Spectral dependencies of radiative and non-radiative components of the decay rate for (a) Ag and (b) Au nanoparticles with 60 nm diameter and 25 nm emitter-particle spacing.

G. Plasmonics to diminish the role of Auger processes

Auger processes develop in quantum wells at high electron-hole pair density. Auger processes are believed to be the major reason for the known commercial quantum-well-based LEDs efficiency droop for higher current.[30–34] Efficiency droop for high currents is a critical issue of solid state lighting efficiency at present. In quantum dots, when more than one electron-hole pair is generated per dot, Auger processes develop as well. Auger processes not only promote non-radiative recombination but can result in quantum dot photoionization.[35,36] Auger recombination is known to lead to quantum dot photodegradation resulting in crucial drop in quantum yield upon operation time of a quantum dot phosphor and possibly will deteriorate the performance of emerging quantum dot colloidal LEDs as well. In II-VI quantum dots used on novel TV sets the core-shell structure is used with very thick, gradient or step-like potential barrier developed by the shell. For colloidal LEDs an anti-Auger design based on multishell and gradient shell around emitting core may not be appropriate since these shells may deteriorate current flow conditions and injection efficiency. For emerging perovskites and carbon dots shell design has not been applied at all.[37–40]

Plasmonics always leads to decay rate enhancement even if it has negative or zero effect on the overall efficiency. Therefore plasmonic effects can be purposefully used to diminish the role of Auger recombination owing to enhanced recombination rate. Thus, not only LED efficiency can be enhanced as our calculations and the first experiments have shown but also the additional positive role should be highlighted of metal nanoparticles to diminish undesirable Auger processes. This positive effect will also increase photostability of phosphors, an issue which needs a special analysis both in theory and in experiments.

III. CONCLUSION AND OUTLOOK

The results presented predict noticeable electroluminescence intensity enhancement which can be implemented in commercial blue LED and in emerging colloidal quantum dot LEDs. Our results bear reasonable agreement with the experimental data available whenever the parameters enabling such a comparison are reported. E. g., 2-fold enhancement[17] at 525 nm for 80 nm Au NPs and 8 nm spacing according to our calculations occurs for $Q_0 = 0.1$. Similar 2-fold enhancement has been reported for the green with Au particles for quantum wells with $Q_0 = 11.7\%$.[22] Very high (20-fold) enhancement reported for OLED[15] results from extremely low $Q_0 = 10^{-7}$. We believe our results will stimulate further experiments and will help to optimize LED design to get better performance.

In addition to convergence with existing experiments, our results suggest some further positive effects of metal nanostructures in LEDs. First, in accordance with the nanoantenna concept and the relevant experimental evidences, metal nanoparticles may alter angular distribution of emitted light and can be used to enhance directionality of light emission.[41–48] Second, plasmonic structures can be used to enhance modulation rate of LEDs[49] and single photon emission rate.[50] Third, plasmonics can be used to diminish LED efficiency droop resulting from Auger recombination. For quantum dot LED, plasmonics promises improvement in photostability preventing photoionization promoted by Auger recombination. Plasmonic effects on Auger processes promise additional positive influence of metal nanoparticles on LED performance and will most probably become a subject of extensive theoretical and experimental analysis on the nearest future.

ACKNOWLEDGMENTS

The work has been supported by BRFFR-TUBITAK #F16T/A-010 and TUBITAK no.115E679, and in part by Singapore National Research Foundation under NRF-NRFI2016-08.

[1] C. D. Geddes, Ed.; *Metal-Enhanced Fluorescence*; Wiley-VHC: New York (2010).
[2] V. V. Klimov, *Nanoplasmonics* (Fizmatlit, Moscow, 2009).
[3] S. V. Gaponenko, *Introduction to Nanophotonics* (Cambridge University Press, Cambridge, 2010).
[4] J. R. Lakowicz, Plasmonics **1**, 5 (2006).
[5] N. Strekal and S. Maskevich, *Reviews in Plasmonics*; C. D. Geddes (Ed.) Springer: Berlin (2010).
[6] O. Kulakovich, N. Strekal, A. Yaroshevich, S. Maskevich, S. Gaponenko, I. Nabiev, U. Woggon, and M. Artemyev, Nano Letters **2**, 1449 (2002).
[7] P. Anger, P. Bharadwaj, and L. Novotny, Phys. Rev. Lett. **96**, 113002 (2006).

[8] P. P. Pompa, L. Martiradonna, A. Della Torre, F. Della Sala, L. Manna, M. De Vittorio, F. Calabi, R. Cingolani, and R. Rinaldi, Nat. Nanotechnol. **1**, 126 (2006).
[9] F. Tam, G. P. Goodrich, B. R. Johnson, and N. J. Halas, Nano Lett. **7**, 496 (2007).
[10] A. Kinkhabwala, Z. Yu, S. Fan, Y. Avlasevich, K. Müllen, and W. E. Moerner, Nat. Photonics **3**, 654 (2009).
[11] D. V. Guzatov, S. V. Vaschenko, V. V. Stankevich, A. Y. Lunevich, Y. F. Glukhov, and S. V. Gaponenko, J. Phys. Chem. C **116**, 10723 (2012).
[12] H. Y. Wang, X. M. Dou, S. Yang, D. Su, D. S. Jiang, H. Q. Ni, Z. C. Niu, and B. Q. Sun, J. Appl. Phys. **115**, 123104 (2014).
[13] D. V. Guzatov and V. V. Klimov, New J. Phys. **13**, 053034 (2011).
[14] J. B. Khurgin, G. Sun, and R. A. Soref, Appl. Phys. Lett. **93**, 021120 (2008).
[15] A. Fujiki, T. Uemura, N. Zettsu, M. Akai-Kasaya, A. Saito, and Y. Kuwahara, Appl. Phys. Lett. **96**, 043307 (2010).
[16] A. Kumar, R. Srivastava, D. S. Mehta, and M. N. Kamalasanan, Org. Electron. **13**, 1750 (2012).
[17] C. Y. Cho, S. J. Lee, J. H. Song, S. H. Hong, S. M. Lee, Y. H. Cho, and S. J. Park, Appl. Phys. Lett. **98**, 051106 (2011).
[18] X. Yang, P. L. Hernandez-Martinez, C. Dang, E. Mutlugun, K. Zhang, H. V. Demir, and X. W. Sun, Adv. Opt. Mater. **3**, 1439 (2015).
[19] N. Y. Kim, S. H. Hong, J. W. Kang, N. Myoung, S. Y. Yim, S. Jung, K. Lee, C. W. Tu, and S. J. Park, RSC Adv. **5**, 19624 (2015).
[20] J. Pan, J. Chen, D. Zhao, Q. Huang, Q. Khan, X. Liu, Z. Tao, Z. Zhang, and W. Lei, Opt. Exp. **24**, A33 (2016).
[21] S. H. Hong, C. Y. Cho, S. J. Lee, S. Y. Yim, W. Lim, S. T. Kim, and S. J. Park, Optics Expr. **21**, 3138 (2016).
[22] C. Y. Cho and S. J. Park, Optics Expr. **24**, 7488 (2016).
[23] S. Gaponenko, H. V. Demir, C. Seassal, and U. Woggon, Optics Expr. **24**, A430–A433 (2016).
[24] L. Su, X. Zhang, Y. Zhang, and A. L. Rogach, Topics Curr. Chem. **374**, 1 (2016).
[25] V. V. Klimov and D. V. Guzatov, Quant. Electron. **37**, 209 (2007).
[26] V. V. Klimov and V. S. Letokhov, Laser Phys. **15**, 61–73 (2005).
[27] P. B. Johnson and R. W. Christy, Phys. Rev. B **6**, 4370 (1972).
[28] G. Lu, T. Zhang, W. Li, L. Hou, J. Liu, and Q. Gon, J. Phys. Chem. C **115**, 15822 (2011).
[29] S. Y. Liu, L. Huang, J. F. Li, C. Wang, Q. Li, H. X. Xu, H. L. Guo, Z. M. Meng, and Z. Y. Li, J. Phys. Chem. C **117**, 10636 (2013).
[30] J. Iveland, L. Martinelli, J. Peretti, J. S. Speck, and C. Weisbuch, Phys. Rev. Lett. **110**, 177406 (2013).
[31] M. Binder, A. Nirschl, R. Zeisel, T. Hager, H.-J. Lugauer, M. Sabathil, D. Bougeard, J. Wagner, and B. Galler, Appl. Phys. Lett. **103**, 071108 (2013).
[32] B. Galler *et al.*, Appl. Phys. Expr. **6**, 112101 (2013).
[33] F. Römer and B. Witzigmann, Optics Expr. **22**, A1440–A1452 (2014).
[34] J. Piprek, Appl. Phys. Lett. **107**, 031101 (2015).
[35] D. I. Chepic, L. Efros Al, A. I. Ekimov, M. G. Ivanov, V. A. Kharchenko, I. A. Kudriavtsev, and T. V. Yazeva, J. Lumin. **47**, 113–127 (1990).
[36] G. E. Cragg and A. L. Efros, Nano Letters **10**, 313 (2010).
[37] P. Docampo and T. Bein, Acc. Chem. Res. **49**, 339 (2016).
[38] S. Gonzalez-Carrero, R. E. Galian, and J. Pérez-Prieto, Opt. Expr. **24**, A285 (2016).
[39] J. Xing, F. Yan, Y. Zhao, S. Che, H. Yu, Q. Zhang, R. Zeng, H. V. Demir, X. Sun, A. Huan, and Q. Xiong, ACS Nano **10**, 6623–6630 (2016).
[40] C. J. Reckmeier, J. Schneider, A. S. Susha, and A. L. Rogach, Optics Expr. **24**, A312–A340 (2016).
[41] G. M. Akselrod, M. C. Weidman, Y. Li, C. Argyropoulos, W. A. Tisdale, and M. H. Mikkelsen, ACS Photonics **3**, 1741–1746 (2016).
[42] T. H. Taminiau, F. D. Stefani, and N. F. van Hulst, New J. Physics **10**, 105005 (2008).
[43] K. L. Tsakmakidis, R. W. Boyd, E. Yablonovitch, and X. Zhang, Optics Expr. **24**, 17916–17927 (2016).
[44] T. Coenen, F. Bernal Arango, A. F. Koenderink, and A. Polman, Nature Commun. **5**, 3250 (2014).
[45] A. G. Curto, G. Volpe, T. H. Taminiau, M. P. Kreuzer, R. Quidant, and N. F. van Hulst, Science **329**, 5994 (2010).
[46] T. Kosako, Y. Kadoya, and H. F. Hofmann, Nature Photon. **4**, 312 (2010).
[47] Z. H. Chen, L. He, Y. Wang, and Z. Gan, IEEE Photonics Journ. **9**, 1 (2017).
[48] R. Bakker, V. Drachev, Z. T. Liu, H. K. Yuan, R. Pedersen, A. Boltasseva, J. J. Chen, J. Irudayaraj, A. Kildishev, and V. Shalaev, New J. Phys. **10**, 125022 (2008).
[49] K. L. Tsakmakidis, R. W. Boyd, E. Yablonovitch, and X. Zhang, Optics Express **24**, 17916 (2016).
[50] S. I. Bozhevolnyi and J. B. Khurgin, 2016 Optica **3**, 1418 (2016).